

# Preconditioning seismic data with 5D interpolation for computing geometric attributes

Satinder Chopra\* and Kurt J. Marfurt†

\*Arcis Seismic Solutions, TGS, Calgary; †The University of Oklahoma, Norman

## Summary

The most common preconditioning of seismic data improves the signal-to-noise ratio of the seismic data by removing spatial noise or enhancing the coherency and alignment of the reflection events, without unnecessary smoothing or smearing of the discontinuities. Although we usually think of removing unwanted features, we can also improve the signal-to-noise ratio by predicting unmeasured signal, such as dead traces and lower-fold areas corresponding to unrecorded offsets and azimuths in the gathers. Missing offsets and azimuths almost always negatively impact pre-stack inversion and AVAz analysis. While missing offsets and azimuths may not result in sufficiently reduced signal-to-noise ratios of stacked data to impair conventional time-structure interpretation, they usually give rise to attribute artifacts. If the inconsistencies in fold follow a regular pattern, we refer to the corresponding attribute pattern as “acquisition footprint”. Acquisition footprint is an undesirable artifact that masks the geologic features or amplitude variations seen on time slices from the seismic data, especially at shallow times. We begin our paper by correlating missing data and areas of low fold to artifacts seen in seismic attributes. We then show how 5D interpolation of missing data prior to pre-stack migration results in more complete gathers resulting in a better balanced stack and the reduction of footprint and other attribute artifacts.

## Introduction

Ideally, one designs a 3D seismic data to properly sample the subsurface geometry in all spatial dimensions: x, y, offset, and azimuth, required by our processing algorithms. In reality, missing shots, platforms and other obstacles, as well as tides and currents that give rise to feathering result in irregular acquisition of marine data. Since the days of the single streamers, the inlines are usually well sampled, while the sampling in the crosslines is usually more coarse. Land acquisition encounters a different suite of obstacles, that coupled with limited recording capacity and greater cost results in small or large ‘holes’ in seismic data coverage. Recording equipment malfunctions and noise bursts during acquisition may add more missing traces to the usable recorded data.

Sparse or missing data create problems for the processing algorithms; early post-stack migration volumes often exhibited aliasing artifacts for poorly sampled data. Pre-stack migration also suffers from aliasing, but the desire to apply pre-stack inversion, AVO, and AVAz demands regularity in the offset and azimuth dimensions for optimum performance. Geometric attributes such as coherence and curvature computed from suboptimally sampled

seismic data give rise to acquisition footprint and other artifacts. We show below how 5D interpolation can aid in many of these instances.

## 5D interpolation

Obviously, the ideal way to fill in the missing data gaps would be to reshoot the data in those areas. Such infill acquisition would be extremely expensive per data point, if the equipment could be made available for such a small time in the field. Such problems have been addressed at the processing stage since the advent of digital processing, whereby adjacent traces are used to populate the missing values. Initial trace replication was superseded by first 2D and later 3D triangular trace interpolation algorithms. These methods, referred to as *local* methods of interpolation as they need localized information for their operation, are fast and easy to implement, but cannot handle large gaps in the data. During the last decade or so, *global* methods for data interpolation have evolved that use farther well-sampled data to populate the missing data. These methods are *multi-dimensional* rather than one-dimensional, operating simultaneously in as many as five different spatial dimensions, and are able to predict the missing data with more accurate amplitude and phase variations. As expected, these methods are compute intensive and have longer run-times than the local methods.

Various multi-dimensional interpolation methods have been proposed by different developers, namely Duijndam et al., (1999), MWNI (Minimum Weighted Norm Interpolation) method by Liu and Sacchi (2004), the ALTF (Anti-leakage Fourier Transform) method by Xu et al. (2005), the POSC (Projection Onto Convex Sets) method by Abma and Kabir (2006), and others by Stein et al., (2010) and Wojslaw et al. (2012). We discuss below the application of the Minimum weighted norm method by Liu and Sacchi (2004).

In this method the interpolation is formulated as an inverse problem where the actual data set is the result of a sampling matrix operation on an unknown fully sampled dataset. The constraint introduced in the problem is that the multidimensional spectrum of the unknown data is the same as that of the original data. This is enforced by a multidimensional Fourier Transform. A cost function is defined and is minimized using standard optimization techniques. Trad (2008, 2009) demonstrated the first commercial implementation of this method.

In Figure 1a we show a representative vertical slice through a merged 3D amplitude volume that has many dead traces. Such

dead traces are seen on other inlines as well. The location of this inline is shown in Figure 2a, where we show a strat-slice through the corresponding coherence volume. The dead traces result in the speckled pattern indicated with yellow ellipses. To regularize the data, 5D interpolation was run on the seismic data prior to migration with the equivalent displays shown in Figures 1b and 2b respectively. Notice in Figure 1b, that not only are the missing traces interpolated, but the overall signal-to-noise ratio and reflector continuity is improved. Similarly, note the absence of the speckles associated with the missing traces and the greater continuity of the distributary system as indicated by the red arrows, although in Figure 2b it appears to be slightly wider than those in Figure 1b indicating slightly less lateral resolution, consistent with an interpolation method.

Whereas coherence attributes measure waveform discontinuities associated with fault offset and channel edges, curvature measures folds, flexures, and differential compaction. In Figure 3 we show a comparison of the principal most-positive curvature (long-wavelength) on the input data and then the same data with 5D interpolation. Missing traces give rise to inaccurate estimates of structural dip which is input to volumetric curvature computations. Ellipses indicate the effect of dead traces on volumetric curvature in Figure 3a. Note the more continuous, better focused lineaments seen on curvature computed from the 5D-interpolated volume in Figure 3b. Figure 4 shows a similar comparison is shown for the principal most-negative curvature (long-wavelength). As with Figure 2, we do however notice slightly less lateral resolution of the attributes computed from the 5D-interpolated data, indicated by yellow arrows in Figure 3b.

The inference we draw from this exercise is that regularization by 5D interpretation yields better focused but less well-defined images. To improve the lateral resolution, we suggest the use of short wavelength version of the principal curvature as shown in Figure 5. Interpretation carried out on such attributes will definitely be more accurate than the one carried out on data without regularization.

Acquisition footprint is also seen suppressed on attributes run on regularized data. In Figure 6b, notice the footprint pattern is suppressed significantly yielding cleaner displays.

### Acquisition footprint suppression

Acquisition footprint is a term we use to define linear spatial grid patterns seen on 3D seismic time slices. These patterns are commonly seen on shallow time slices or horizon amplitude maps as striations masking the actual amplitude anomalies under consideration for stratigraphic interpretation, AVO analysis, and reservoir attribute studies (Marfurt et al., 1998). An acquisition footprint may be present due to various reasons, but two general types of footprint can be distinguished: those depending on the details of the acquisition geometry, and those arising from signal processing problems (Drummond et al., 2000). The choice of any

acquisition design is characterized by a particular distribution of fold, offset, and azimuth. Apart from some variation in the taper zone, the fold for most common geometries should be uniform for all seismic bins. However, the offset and azimuth distribution can vary from bin to bin, or can be uniform in the inline direction and irregular in the cross-line direction. Such variations can lead to undesirable effects on the reflected signal. Deviations from a regular geometry pattern, such as inaccessible patches within a 3D survey area that are under human habitation or the location of a power station, can be responsible for such variation.

Very often economic considerations compel coarse sampling in 3D data acquisition, which can cause artifacts during processing. Coarse spatial sampling leads to aliasing, and aliased steeply dipping noise resulting from ground roll or multiples, for example, creates artifacts. Aliased noise can be accentuated during processing and leak into the stack volumes as spatially periodic events, forming an acquisition footprint. Other processes that tend to accentuate footprints are residual NMO caused by incorrect velocities, systematic errors in computed offsets, or amplitude variations caused by inadequate 3D DMO formulation (Walker et al., 1995; Budd et al., 1995), 3D pre-stack migration, signal enhancements based on  $f$ - $x$ - $y$  random noise attenuation, and coherency filtering (Moldoveanu et al., 1999).

An acquisition footprint, whether resulting from acquisition design or accentuation during processing, is a nuisance for the interpreter. Efforts are sometimes made to prevent accentuation of the footprint during processing, usually by adopting interpolation or extrapolation to remedy the 'sparseness' of the input data volumes before applying multi-channel processes. If interpolation is computationally prohibitive, we can resort to trace mixing, which tends to minimize the footprint effect at the risk of reducing lateral resolution. Gulunay (1999) found that wavenumber domain filtering based on the acquisition design often works. A similar filtering method for non-orthogonal geometries has been suggested by Soubras (2001).

Chopra and Larsen (2000) suggested a similar way of dealing with the acquisition footprint, which is to analyze the footprint-contaminated post-stack migrated data, time slice by time slice, in the  $kx$ - $ky$  wavenumber domain. Apart from  $kx$ - $ky$  filtering, spatially adaptive methods using wavelet transforms have been suggested for highly irregular footprint (Jervis, 2006; Cvetkovic et al., 2007). Al-Bannagi et al. (2005) proposed a method using principal component analysis. By animating through the seismic as well as the corresponding coherence slices, the interpreter can define the change in footprint with depth.

As 5D interpolation discussed above regularizes the geometry of the seismic data, it addresses the root cause of the footprint arising due to the acquisition irregularities. In Figure 6 we show time slices at 158 ms where the acquisition footprint appears prominently on the coherence attribute as striations in the NE-SW direction masking the reflection detail behind them. Figure 6b

shows the equivalent coherence slice after 5D regularization exhibiting considerable improvement in data quality. Similarly, Figure 7 shows cleaner and clearer curvature displays that one can derive from the data after 5D regularization and resulting in a more confident interpretation.

**Conclusions**

Seismic data usually have geometry regularization issues that give rise to artifacts on geometric attribute displays. 5D interpolation methods adopted during processing help address issues such as

missing data pockets and acquisition footprint striations. Coherence and curvature attributes computed on regularized seismic data yield displays clear of these artifacts and so lead to more confident displays.

**Acknowledgements**

We thank Arcis Seismic Solutions, TGS, for encouraging this work and for permission to present these results. The first author acknowledges the processing division of Arcis Seismic Solutions for the processing of seismic data with 5D interpolation.

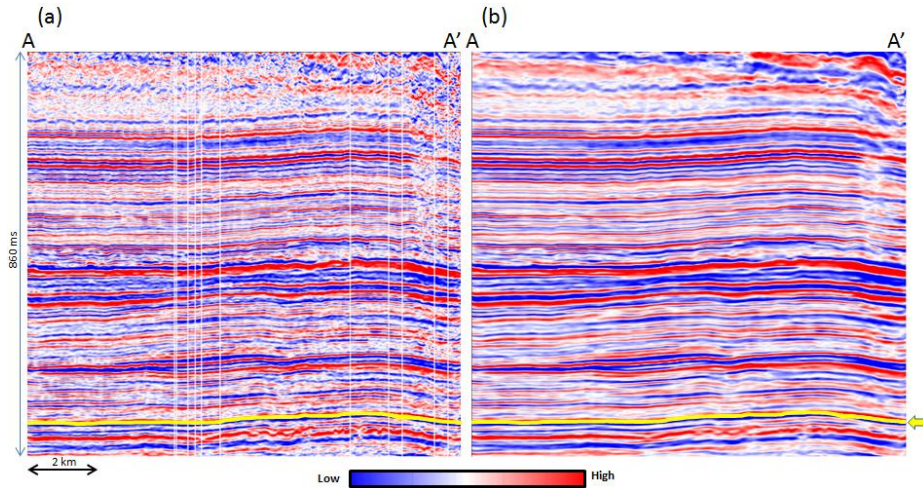


Figure 1: Vertical slices through the seismic amplitude volume (a) before, and (b) after 5D interpolation.

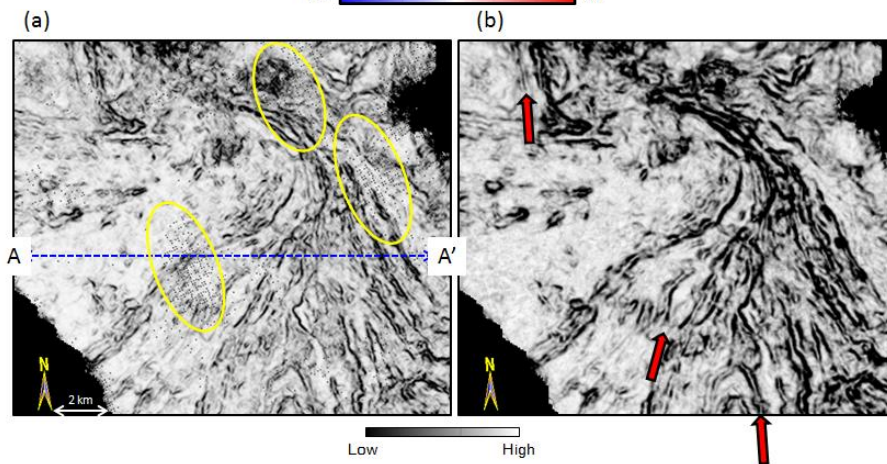


Figure 2: Stratal slices 32 ms below the yellow horizon shown in Figure 1 through coherence volumes computed from amplitude data (a) before, and (b) after 5D interpolation.

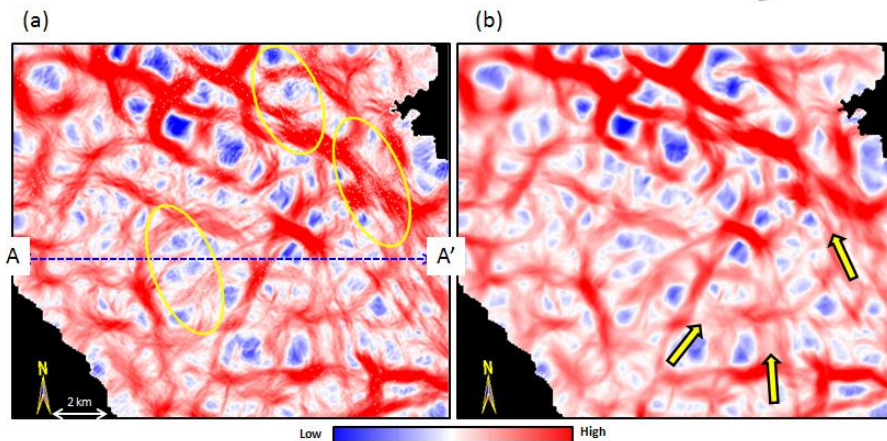


Figure 3: Stratal slices 32 ms below the yellow horizon shown in Figure 1 through principal most-positive curvature (long-wavelength) volumes computed from seismic amplitude data (a) before, and (b) after 5D interpolation.

Downloaded 10/09/13 to 205.196.179.238. Redistribution subject to SEG license or copyright; see Terms of Use at http://library.seg.org/

Downloaded 10/09/13 to 205.196.179.238. Redistribution subject to SEG license or copyright; see Terms of Use at <http://library.seg.org/>

Preconditioning seismic data with 5D interpolation for computing geometric attributes

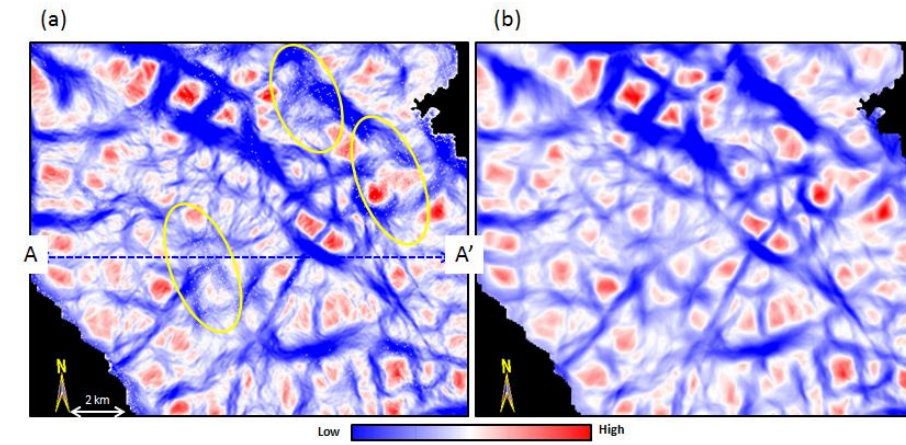


Figure 4: Stratal slices 32 ms below the yellow horizon shown in Figure 1 from principal most-negative curvature (long-wavelength) volumes computed from seismic amplitude data (a) before, and (b) after 5D interpolation.

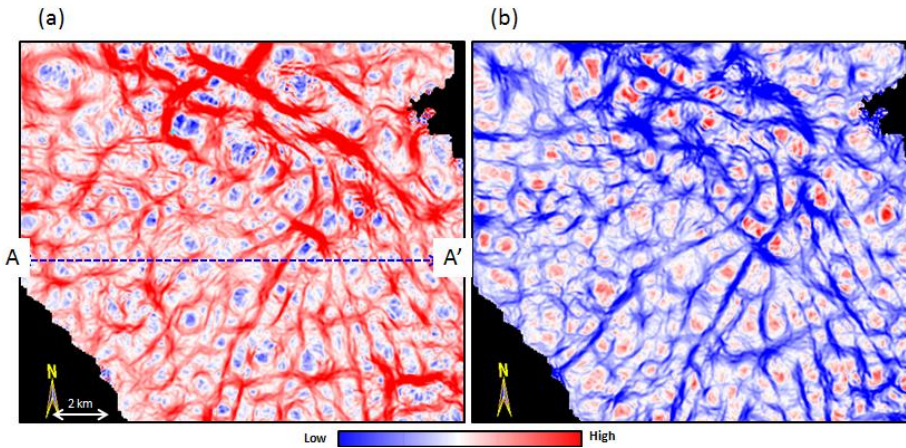


Figure 5: Stratal slices 32 ms below the yellow horizon shown in Figure 1 from (a) principal most-positive curvature (short-wavelength) and (b) principal most-negative curvature (short-wavelength) volumes run on input data with 5D interpolation.

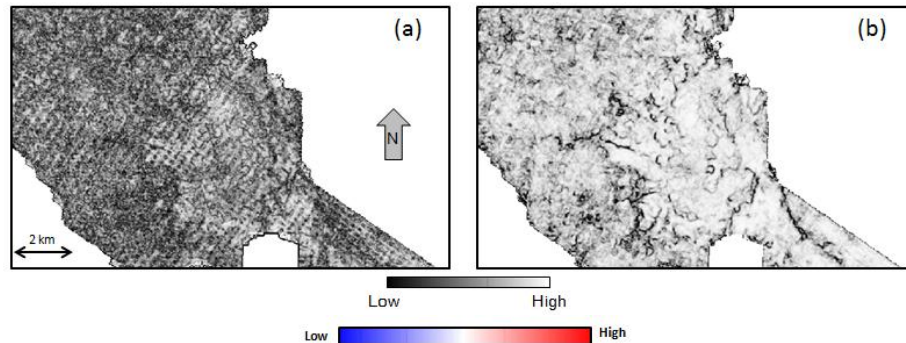


Figure 6: Time slices at 158 ms through coherence volumes computed from amplitude data (a) before, and (b) after 5D interpolation.

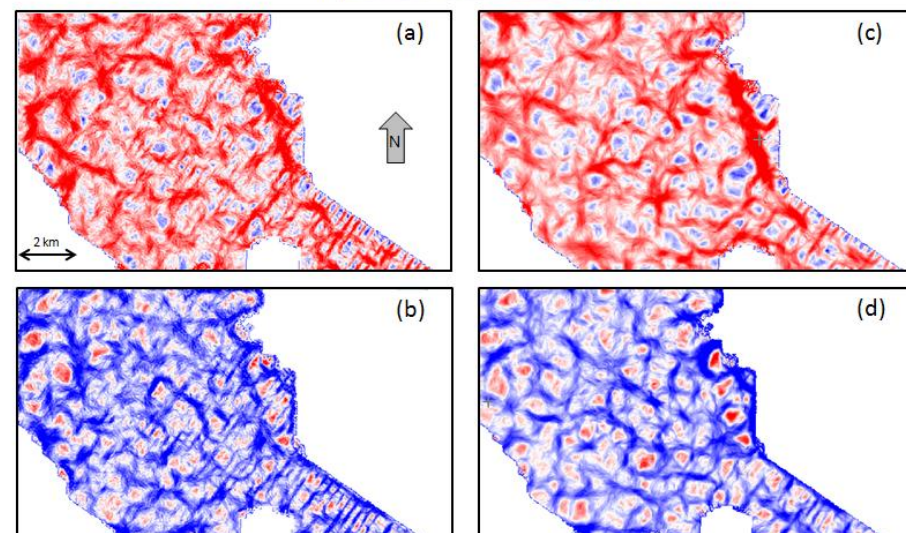


Figure 7: Time slices at 158 ms the (a) most-positive curvature (long-wavelength) and (b) most-negative curvature (long-wavelength) volumes run on the uninterpolated input data. Equivalent time slices through the (c) most-positive curvature (long-wavelength) and (d) most-negative curvature (long-wavelength) volumes run on the 5D-interpolated input data.

<http://dx.doi.org/10.1190/segam2013-0169.1>

#### EDITED REFERENCES

Note: This reference list is a copy-edited version of the reference list submitted by the author. Reference lists for the 2013 SEG Technical Program Expanded Abstracts have been copy edited so that references provided with the online metadata for each paper will achieve a high degree of linking to cited sources that appear on the Web.

#### REFERENCES

- Abma, R., and N. Kabir, 2006, 3D interpolation of irregular data with a POCS algorithm: *Geophysics*, **71**, no. 6, E91–E97, <http://dx.doi.org/10.1190/1.2356088>.
- Al-Bannagi, M., K. Fang, P. G. Kelamis, and G. S. Douglass, 2005, Acquisition footprint suppression via the truncated SVD technique: case studies from Saudi Arabia: *The Leading Edge*, **24**, 832–834, <http://dx.doi.org/10.1190/1.2032259>.
- Budd, A. J. L., K. Hawkins, A. R. Mackewn, and J. W. Ryan, 1995, Marine geometry for optimum 3D seismic imaging: 57th EAGE Conference and Exhibition, Extended Abstracts, B030.
- Chopra, S., and G. Larsen, 2000, Acquisition footprint — its detection and removal: *CSEG Recorder*, **25**, no. 8, 16–20.
- Cvetkovic, M., S. Falconer, K. J. Marfurt, and S. C. Perez, 2007, 2D stationary wavelet-based acquisition footprint suppression: 77th Annual International Meeting, SEG, Expanded Abstracts, 2590–2593.
- Drummond, J. M., A. J. L. Budd, and J. W. Ryan, 2000, Adapting to noisy 3D data – attenuating the acquisition footprint: 70th Annual International Meeting, SEG, Expanded Abstracts, 9–12.
- Duijndam, A. J. W., M. A. Schonewille, and C. O. H. Hindriks, 1999, Reconstruction of band-limited signals, irregularly sampled along one spatial direction: *Geophysics*, **64**, 524–538, <http://dx.doi.org/10.1190/1.1444559>.
- Gulunay, N., 1999, Acquisition geometry footprints removal: 69th Annual International Meeting, SEG, Expanded Abstracts, 637–640.
- Jervis, M., 2006, Edge preserving filtering on 3D seismic data using complex wavelet transforms: 76th Annual International Meeting, SEG, Expanded Abstracts, 2872–2876.
- Liu, B., and M. Sacchi, 2004, Minimum weighted norm interpolation of seismic records: *Geophysics*, **69**, 1560–1568, <http://dx.doi.org/10.1190/1.1836829>.
- Moldoveanu, N., S. Ronen, and S. Mitchell, 1999, Footprint analysis of land and TZ acquisition geometries using synthetic data: 69th Annual International Meeting, SEG, Expanded Abstracts, 641–644.
- Soubaras, R., 2002, Attenuation of acquisition footprint for nonorthogonal 3D geometries: 72nd Annual International Meeting, SEG, Expanded Abstracts, 2142–2145.
- Stein, J. S., S. Boyer, K. Hellman, and J. Weigant, 2010, Application of POCS interpolation to exploration: 80th Annual International Meeting, SEG, Expanded Abstracts, 2013–2016.
- Trad, D., 2008, Five-dimensional seismic data interpolation: 78th Annual International Meeting, SEG, Expanded Abstracts, 978–982.
- Trad, D., 2009, Five-dimensional seismic data interpolation: CSEG/CSPG/CWLS Convention, Expanded Abstracts, 689–692.

- Walker, C. D. T., A. R. Mackewn, A. J. L. Budd, and J. W. Ryan, 1995, Marine 3D geometry design for optimum acquisition system response: 57th EAGE Conference and Exhibition, Extended Abstracts, B029.
- Wojslaw, R., J. A. Stein, and T. Langston, 2012, 5D semblance-based interpolator in exploration-theory and practice: 74th EAGE Conference and Exhibition, Extended Abstracts, B024.
- Xu, S., Y. Zhang, and G. Lambare, 2005, Recovering densely and regularly sampled 5D seismic data for current land acquisition: 67th EAGE Conference and Exhibition, Extended Abstracts, W024.